

Maximally entangled gapped ground state of lattice fermions

David L. Feder*

Institute for Quantum Information Science, University of Calgary, Alberta T2N 1N4, Canada

(Dated: September 15, 2018)

Entanglement between the constituents of a quantum system is an essential resource in the implementation of many quantum processes and algorithms. Indeed, universal quantum computation is possible by measuring individual qubits comprising highly entangled ‘cluster states.’ In this work it is shown that the unique gapped ground state of non-interacting fermions hopping on a specially prepared lattice is equivalent to a cluster state, where the entanglement between qubits results solely by fermionic indistinguishability and antisymmetry. A deterministic strategy for universal measurement-based quantum computation with this resource is described. Because most matter is composed of fermions, these results suggest that resources for quantum information processing might be generic in Nature.

I. INTRODUCTION

In measurement-based quantum computation (MBQC) [1], an algorithm proceeds entirely by making projective measurements of successive particles (qubits or qudits) comprising some highly entangled ‘resource state.’ While two-dimensional cluster states are known to be universal resources for MBQC [2], it has been proven that they cannot be the unique ground states of any qubit Hamiltonian involving at most two-body interactions [3]. Because two-body interactions are generic in Nature, this limitation has driven a search for other universal resource states that might exist as the ground state of a physical system. An alternative representation of MBQC using Matrix Product States (MPS) [4] in one dimension and its extension to higher dimensions using Projected Entangled Pair States (PEPS) [5, 6] indicates that there are many states with much less entanglement than the cluster states that are nevertheless universal resources [7–9]. Unfortunately, the fraction of useful resource states is known to be exponentially small in the number of physical qubits [10, 11]. Worse, it is presently unknown if any of these states is the unique, gapped ground state of any physically realizable Hamiltonian. By relaxing various assumptions, it is possible to define accessible Hamiltonians whose ground states are universal resources for MBQC. One example is a system of spin-5/2 qudits on the hexagonal lattice with two-body interactions, where the ground state is unique and gapped [12]. Another is the AKLT model of an antiferromagnet [13] with spin-3/2 qudits on the hexagonal lattice, which is gapped but degenerate [14, 15].

An unrelated strategy for MBQC was devised for indistinguishable free fermions using beam splitters and charge detectors [16] in analogy with non-deterministic linear optical quantum computation [17]. In fact, cluster states can be dynamically generated using this approach [18]. The relationship between free fermions and

entanglement has subsequently been the subject of extensive investigations [19, 20]. More recently, the relationships between fermions and quantum information are being explored [21–24]. In particular, it has been shown that quantum circuits composed only of match-gates [25, 26] (which are closely related to non-interacting fermions) can generate entanglement yet are efficiently classically simulatable unless supplemented by an apparently trivial resource, the unentangling SWAP gate [22].

In this work, the ideas above are combined to show that the non-degenerate and gapped ground state of a non-interacting fermionic lattice Hamiltonian is equivalent to a cluster state comprised of qubits, under the conditions that any site has at most one fermion and the lattice is exactly half-filled. The qubit registers then correspond to the occupation of lattice sites. The entanglement is a direct consequence of fermionic indistinguishability and antisymmetry. Measurements correspond to detecting the presence or absence of a fermion in a lattice site, equivalent to a restriction to the computational basis. In order to simulate a universal quantum computer, one must rotate the measurement from the computational Z basis into the X or Y basis via the application of a Hadamard gate H or a \sqrt{X} operation (here X , Y , and Z represent the Pauli matrices). Surprisingly, in the fermionic model these gates cannot be directly implemented because of the intrinsic entanglement; rather, an additional lattice must be introduced that allows two fermions encoding different qubits to interact, thereby cancelling the effects of the fermionic antisymmetry. Fermionic systems therefore invert the usual quantum computing paradigm, in that entanglement is intrinsic but general single-qubit operations require particle interactions.

The manuscript is organized as follows. A review of cluster states and the measurement-based model for universal quantum computation using them is briefly reviewed in Sec. II. Sec. III introduces the main fermionic model, and demonstrates that in principle the ground state is a universal resource for MBQC. The implementation of a universal set of quantum gates by measurements is discussed in Sec. IV, where it is shown that interactions and additional potentials are required. The implications of the results are summarized in Sec. V.

* dfeder@ucalgary.ca

II. REVIEW OF CLUSTER-STATE QUANTUM COMPUTATION

The stabilizers of a given state $|\psi\rangle$ are the operators S_i for which one satisfies $S_i|\psi\rangle = |\psi\rangle$ for each i . If $|\psi\rangle$ is a stabilizer state, then its Hilbert space dimension exactly coincides with the number of stabilizers S_i . A useful class of stabilizer states are known as graph states, where qubits are represented by vertices and maximal two-qubit entanglement between two qubits is represented by an edge connecting the vertices. For a generic graph state $|g\rangle$ on N qubits, the N generators for the 2^N -dimensional group of stabilizers are given by the separable operators $S_i = X_i \otimes_{j \in \mathcal{N}(i)} Z_j$, where $\mathcal{N}(i)$ signifies the neighbourhood of site (qubit) i , and where X_i , Y_i , and Z_i denote Pauli matrices acting on qubit i . A Hamiltonian that is guaranteed to have $|g\rangle$ as the lowest energy state (with eigenvalue $-N\tau$) is therefore

$$\hat{H} = -\tau \sum_{i=1}^N S_i = -\tau \sum_{i=1}^N X_i \bigotimes_{j \in \mathcal{N}(i)} Z_j. \quad (1)$$

For cluster states, in which the qubits are arranged on a regular lattice, the coordination number is two and four for one-dimensional (1D) and two-dimensional (2D) lattices, respectively. This implies that the Hamiltonian above consists of three-spin and five-spin operators in 1D and 2D, respectively. In fact, this number has been proven to be a minimum, i.e. there is no Hamiltonian having all terms with fewer spin operations that can have $|g\rangle$ as a (non-degenerate) ground state [3].

In the one-dimensional case, the cluster ground state is

$$|C_N\rangle \equiv \prod_{i=1}^{N-1} CZ_{i,i+1}|+\rangle^{\otimes N}, \quad (2)$$

where $CZ_{i,j} \equiv \text{diag}(1, 1, 1, -1)$ is the maximally entangling controlled-phase gate and $|+\rangle = (|0\rangle + |1\rangle)/\sqrt{2}$ is the $+1$ eigenstate of the X operator. In this representation, it is evident that the cluster state is highly entangled: each qubit is maximally entangled with its neighbor. The excited states correspond to $\prod_{j=1}^N Z_j^{k_j} |C_N\rangle$, where $k_j \in \{0, 1\}$, and have energies $(-N + \ell)\tau$ with $\ell \in \{1, \dots, 2N\}$. The energy gap to the first excited state is therefore τ , constant in the thermodynamic limit.

To perform universal quantum computation, it suffices to measure qubits in successive columns of the 2D lattice in the $HR_Z(\theta)$ basis, where H and $R_Z(\theta) = \exp(-i\frac{\theta}{2}Z)$ are the Hadamard operator and rotation by an angle θ around the Z -axis, respectively:

$$H = \frac{1}{\sqrt{2}} \begin{pmatrix} 1 & 1 \\ 1 & -1 \end{pmatrix}; \quad R_Z(\theta) = \begin{pmatrix} e^{-i\theta/2} & 0 \\ 0 & e^{i\theta/2} \end{pmatrix}$$

This corresponds to measurements in a basis spanned by the vectors $|+\theta\rangle = \frac{1}{\sqrt{2}}(1 + e^{-i\theta})$ and

$|-\theta\rangle = \frac{1}{\sqrt{2}}(1 - e^{-i\theta})$; alternatively, the operation $HR_Z(\theta)$ is first applied to the qubit, and then it is measured in the computational basis. In both cases, the result of measuring qubit 1 of a linear cluster state with N qubits is $|m\rangle_1 \otimes [X^m HR_Z(\theta)]_2 |+\rangle^{\otimes(N-1)}_{2,3,\dots,N}$, where $m = \{0, 1\}$ is the measurement outcome and the subscript is the qubit index. The presence of the X gate reflects the probabilistic nature of the measurement outcome. Three successive measurements with three independent angles (adapted to previous measurements because of the possible presence of an X gate) suffices to teleport an arbitrary single-qubit gate in 1D cluster states; a universal set of gates results in 2D cluster states [1].

III. ENTANGLEMENT IN LATTICE FERMIONS

A. Fermionic model

The fermionic model employed in this work is inspired by experiments with ultracold atomic gases. Numerous groups have confined both bosonic and fermionic atoms in periodic potentials formed from interfering lasers, known as optical lattices [27, 28]. These lattices can confine different spin components of the same bosonic species in independent, overlapping optical lattices [29, 30]. The structure of these lattices is highly flexible [31], and periodic double-well potentials for bosons have been the subject of particularly intense investigations [32–36]. In another recent development, an ultracold gas consisting of a mixture of three different spin components of the fermionic atom ${}^6\text{Li}$ has been realized in an optical trap [37, 38]. Ultracold fermionic gases of both ${}^{40}\text{K}$ and ${}^6\text{Li}$ have been loaded into periodic optical lattices with highly controllable geometries and trapping parameters [39–42]. It is reasonable to assume that these various techniques could be combined in the future, with multi-component fermions in three overlapping double-well optical lattices, each confining a different spin component.

Consider the potentials depicted in Fig. 1(a), corresponding to three overlapping one-dimensional two-site lattices. It is assumed that each sublattice can confine only one particular spin projection of a fermion with pseudospin $s = 1$ (corresponding to real spin $s \geq 3/2$ with all but three spin projections frozen out); the spin projections will be labeled \uparrow , o , and \downarrow . The potential shown as a black curve is assumed to confine only the spin o , and could be obtained using two potentials with amplitudes $V_{1,o}$ and $V_{2,o}$ and with one wavelength λ half as large as another:

$$V_o(x) = V_{1,o} \cos^2\left(\frac{2\pi x}{\lambda}\right) + V_{2,o} \cos^2\left(\frac{\pi x}{\lambda}\right).$$

Likewise, the potentials seen by the \uparrow and \downarrow spin projections (green and red curves in Fig. 1(a), respectively)

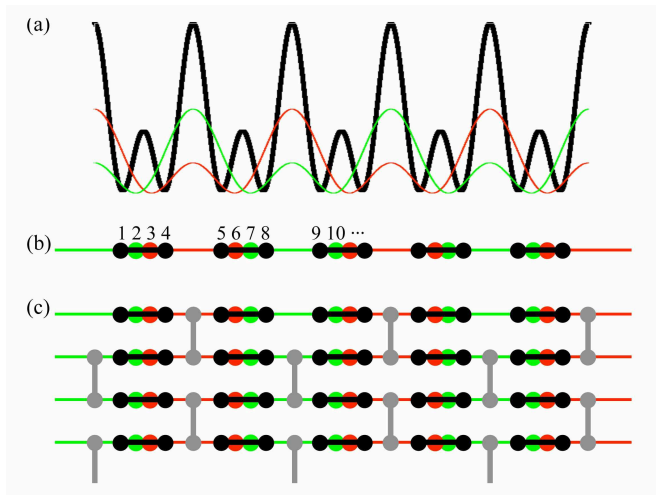


FIG. 1. (Color online) Depiction of the fermionic leapfrog model. Each spin projection experiences a unique spatially-dependent potential energy, shown as the black, red (dark gray), and green (light gray) curves in (a). Assuming that the higher potential barriers are effectively impenetrable, one obtains the hopping model in (b), with three overlapping double-well sublattices. A two-dimensional extension of the one-dimensional model is shown in (c).

would be generated by wavelengths that were twice as long as for projection o , and offset relative to each other:

$$V_{\uparrow}(x) = V_{1,\uparrow} \cos^2\left(\frac{\pi(x-\lambda)}{\lambda}\right) + V_{2,\uparrow} \cos^2\left(\frac{\pi(x-\lambda)}{2\lambda}\right);$$

$$V_{\downarrow}(x) = V_{1,\downarrow} \cos^2\left(\frac{\pi x}{\lambda}\right) + V_{2,\downarrow} \cos^2\left(\frac{\pi x}{2\lambda}\right).$$

The relative height of the barriers is then set by the ratio $V_{1,\sigma}/V_{2,\sigma}$. Within the tight-binding approximation, assuming the atoms can only tunnel through the lower barrier of a given sublattice, the Hamiltonian becomes

$$\hat{H} = - \sum_{j=0}^{N-1} \left(\tau_{\uparrow} f_{8j+2,\uparrow}^{\dagger} f_{8j-1,\uparrow} + \tau_o f_{4j+4,o}^{\dagger} f_{4j+1,o} + \tau_{\downarrow} f_{8j+6,\downarrow}^{\dagger} f_{8j+3,\downarrow} + \text{H.c.} \right), \quad (3)$$

where $f_{i,\sigma}^{\dagger}$ ($f_{i,\sigma}$) creates (annihilates) a fermion with spin projection σ at site i . The τ_{σ} correspond to hopping amplitudes, the exact values of which are unimportant for the present work.

There is no tunneling permitted between different sublattices, but nevertheless fermions with different spin projections must anticommute if the sublattices overlap: if a fermion with one spin projection tunnels past a fermion with another spin projection, the total wavefunction picks up a negative sign. This is because it is impossible to distinguish if the fermions interchanged their spin labels (switching places) during the transit, or remained the same. At the same time, it is unnecessary to impose antisymmetrization on fermions that can never

overlap in practice. For example, a o -projection fermion in site 1 in Fig. 1(b) needs to be antisymmetrized only with fermions in sites 2, 3, and 4; the tunneling barrier between sites 4 and 5 is assumed to be so large as to prevent any tunneling for o -spin projection atoms.

The relative strengths of the tunneling amplitudes are not important for the ground state, as long as they are all non-zero. One may assume that the system is given sufficiently long to equilibrate compared to the tunneling rates. Thus one may choose $\tau_o = \tau_{\uparrow} = \tau_{\downarrow} \equiv \tau$ without loss of generality. The Hamiltonian (3) can be further simplified by noting that fermions with a given spin projection are constrained to their respective sublattices. The spin-projection index can therefore be suppressed, corresponding to spinless (fully polarized) fermions. One then obtains the equivalent ‘leapfrog’ Hamiltonian

$$\hat{H} = -\tau \sum_{j=0}^{N-1} \left(f_{2j+4}^{\dagger} f_{2j+1} + f_{2j+1}^{\dagger} f_{2j+4} \right), \quad (4)$$

which is the central model of the current work, and is depicted graphically in Fig. 1(b). Though the Hamiltonian appears to involve third-nearest neighbor hopping, it is in fact obtained by nearest-neighbor hopping on an array of three overlapping two-site sublattices.

B. Cluster ground state

Consider only the case where each spinless sublattice is exactly half-filled: each connected double-well indexed by j contains exactly one fermion, $n_{2j+1} + n_{2j+4} \equiv 1$. Mathematically, this could be accomplished by applying a suitable projector to the Hamiltonian (4). In an experiment with ultracold atoms, such a configuration could be obtained by detecting and selectively moving or removing single atoms [43–47].

Making use of the Jordan-Wigner transformation

$$f_j = \frac{1}{2} \bigotimes_{k=1}^{j-1} Z_k \otimes (X_j + iY_j);$$

$$f_j^{\dagger} = \frac{1}{2} \bigotimes_{k=1}^{j-1} Z_k \otimes (X_j - iY_j), \quad (5)$$

the Hamiltonian (4) may be expressed in the spin representation:

$$\hat{H} = -\frac{\tau}{2} \sum_{j=0}^{N-1} Z_{2j+2} Z_{2j+3} (X_{2j+1} X_{2j+4} + Y_{2j+1} Y_{2j+4}), \quad (6)$$

which is four-local in marked contrast to that in the fermion representation. Because of the half-filling restriction, the ground state only involves states with Hamming weight N and therefore only involves combinations of the encoded registers

$$|0_j\rangle \equiv |1_{2j+1} 0_{2j+4}\rangle = f_{2j+1}^{\dagger} |\mathcal{O}\rangle;$$

$$|1_j\rangle \equiv |0_{2j+1} 1_{2j+4}\rangle = f_{2j+4}^{\dagger} |\mathcal{O}\rangle,$$

where the state $|\mathcal{O}\rangle$ represents the particle vacuum. In other words, the $|\underline{0}_j\rangle$ register has the single fermion on the first site of a given double-well indexed by j , while the $|\underline{1}_j\rangle$ register corresponds to the fermion in the second site.

One can introduce an encoded basis where the operators become $(X_{2j+1}X_{2j+4} + Y_{2j+1}Y_{2j+4})/2 \equiv \underline{X}_j$, $I_{2j+1}Z_{2j+4} \equiv \underline{Z}_j$, and $Z_{2j+1}I_{2j+4} \equiv -\underline{Z}_j$ (recall the half-filling condition), i.e. $\underline{X}_j|\underline{0}_j\rangle = |\underline{1}_j\rangle$ and vice versa, $\underline{Z}_j|\underline{0}_j\rangle = |\underline{0}_j\rangle$, and $\underline{Z}_j|\underline{1}_j\rangle = -|\underline{1}_j\rangle$. Using $Z_{2j+2} = I_{2(j-1)+1}Z_{2(j-1)+4} = \underline{Z}_{j-1}$ and $Z_{2j+3} = Z_{2(j+1)+1}I_{2(j+1)+4} = -\underline{Z}_{j+1}$, the Hamiltonian (6) in the encoded basis becomes

$$\hat{H} = \tau \sum_{j=1}^{N-1} \underline{Z}_{j-1} \underline{X}_j \underline{Z}_{j+1} - \tau \underline{Z}_{N-1} \underline{X}_N, \quad (7)$$

with $\underline{Z}_0 = \underline{I}_1$. Applying the unitary transformation \underline{Z}_j for all $j \in \{1, N-1\}$ performs the maps $\underline{X}_j \rightarrow -\underline{X}_j$, transforming (7) into exactly the same Hamiltonian as the one-dimensional cluster-state Hamiltonian on N qubits, Eq. (1). The ground state of Hamiltonian (7) is therefore immediately obtained by comparing with the usual cluster state, Eq. (2):

$$|\text{g.s.}\rangle = \prod_{j=1}^{N-1} \underline{Z}_j \underline{CZ}_{j,j+1} |+\rangle^{\otimes N},$$

where $|+\rangle \equiv (|\underline{0}\rangle + |\underline{1}\rangle) / \sqrt{2}$, and the encoded entangling gate is defined as $\underline{CZ}_{j,j+1} \equiv \text{diag}(1, 1, 1, -1)$ in the space spanned by the vectors $|\underline{0}_j \underline{0}_{j+1}\rangle$, $|\underline{0}_j \underline{1}_{j+1}\rangle$, $|\underline{1}_j \underline{0}_{j+1}\rangle$, and $|\underline{1}_j \underline{1}_{j+1}\rangle$. It is clear that the ground state is equivalent to the one-dimensional cluster state, where each qubit is maximally entangled to its neighbor. This entanglement is a direct consequence of fermionic antisymmetry and indistinguishability. The excitations correspond to \underline{Z}_i operations on the ground state, which cost energy τ . The energy gap is therefore τ , independent of system size.

C. Example: two qubits

Consider the consequences of measuring the position of one of the two fermions in a two-qubit fermionic cluster state. Suppose that the entire system consisted of sites 1, 3, 4, and 6 in Fig. 1(b). In the absence of inert fermions in the unpaired sites 2 and 5, these sites can be ignored, and the ground state of the Hamiltonian (4) is maximally entangled:

$$\begin{aligned} |\text{g.s.}\rangle &= \frac{1}{2} \left(f_1^\dagger + f_4^\dagger \right) \left(f_3^\dagger + f_6^\dagger \right) |\mathcal{O}\rangle_{1,3,4,6} \\ &= \frac{1}{2} (|1100\rangle + |1001\rangle - |0110\rangle + |0011\rangle)_{1,3,4,6} \\ &= \underline{Z}_1 \underline{CZ}_{12} |++\rangle. \end{aligned} \quad (8)$$

In the Fermi-occupation notation, the ground state appears to be separable; however, this ignores the fact that

fermions on sites 3 and 4 must anticommute if there is any chance that these fermions can interchange. Consequently, defining the fermionic occupation states in the natural ordering by increasing label $|0110\rangle_{1,3,4,6} = f_3^\dagger f_4^\dagger |\mathcal{O}\rangle_{1,3,4,6}$, a negative sign appears on the second line above. If the fermions on site-pairs $\{1, 4\}$ and $\{3, 6\}$ could never overlap (i.e. there was an impenetrable barrier between them), then the state would be truly separable and no explicit antisymmetrization would be required.

Measurement of the first qubit in encoded state $|\underline{0}_1\rangle$ corresponds to the application of the projector $(\mathcal{M}_1)_1 = |1_1 0_4\rangle\langle 1_1 0_4| = f_1^\dagger |\mathcal{O}\rangle\langle \mathcal{O}| f_1$, yielding

$$(\mathcal{M}_1)_1 |\text{g.s.}\rangle = \frac{1}{\sqrt{2}} [|1100\rangle + |1001\rangle] = |\underline{0}+\rangle.$$

Likewise, applying the other projector $(\mathcal{M}_2)_1 = |0_1 1_4\rangle\langle 0_1 1_4| = f_4^\dagger |\mathcal{O}\rangle\langle \mathcal{O}| f_4$ yields the state

$$\begin{aligned} (\mathcal{M}_2)_1 |\text{g.s.}\rangle &= \frac{1}{\sqrt{2}} [-|0110\rangle + |0011\rangle] \\ &= -\underline{Z}_1 |\underline{1}+\rangle = -|\underline{1}-\rangle. \end{aligned}$$

The dependence of the second encoded qubit's output state on the outcome of the first encoded qubit's measurement is a direct consequence of the entanglement of the original fermionic state.

It is important to note, and easy to verify, that this result doesn't depend on how one labels the sites. If the two double-sites were instead labeled $\{1, 3\}$ and $\{4, 6\}$, so that no negative sign appeared in the ground state (8), the same states would still be obtained after measurement. This is because the result of the measurement operation on the double-site $\{1, 3\}$ explicitly depends on the possible existence of a fermion at the intervening site 4. If instead the two double-wells were disconnected (non-overlapping), then there would be no intervening site with which to anticommute, and therefore no dependence of the output on the measurement outcome. In short, the entanglement arises from the fundamental requirement that fermions on the sites 3 and 4 must anticommute when there is the potential for these wavefunctions to overlap.

IV. UNIVERSAL MEASUREMENT-BASED QUANTUM COMPUTATION WITH LATTICE FERMIONS

A. Single-qubit operations with fermions

In order to perform universal gate teleportation using the encoded cluster state, Eq. (10) in the manuscript, it is important to derive expressions for the encoded \underline{X} , \underline{Y} , and \underline{Z} -rotations, Hadamard operator \underline{H} , and measurement operators that one would need to apply in order to teleport gates with fermions. The encoded \underline{Z} -rotation is

straightforward:

$$\begin{aligned}\underline{R}_Z(\theta)_j &= \exp\left(-i\underline{Z}_j\frac{\theta}{2}\right) = \exp\left(-iZ_{2j+4}\frac{\theta}{2}\right) \\ &= \cos\left(\frac{\theta}{2}\right) - i\sin\left(\frac{\theta}{2}\right)(1 - 2n_{2j+4}),\end{aligned}$$

where $1 - 2n_{2j+4} = \underline{Z}_j$ is the encoded Z operator. Because $n_{2j+4} = 1 - n_{2j+1}$ an equivalent expression would

be

$$\underline{R}_Z(\theta)_j = \cos\left(\frac{\theta}{2}\right) + i\sin\left(\frac{\theta}{2}\right)(1 - 2n_{2j+1}).$$

Thus, $\underline{R}_Z(\theta) = e^{-i\theta/2}$ if the fermion is in the first site and $\underline{R}_Z(\theta) = e^{i\theta/2}$ if it is in the second, as expected from the qubit encoding. To obtain the encoded \underline{X} -rotation, one can make use of the relations

$$\begin{aligned}\underline{X}_j &= (1 - 2n_{2j+2})(1 - 2n_{2j+3}) \\ &\quad \times \left(f_{2j+4}^\dagger f_{2j+1} + f_{2j+1}^\dagger f_{2j+4}\right),\end{aligned}\quad (9)$$

and $\underline{X}_j^2 = n_{2j+1}(1 - n_{2j+4}) + n_{2j+4}(1 - n_{2j+1}) = n_{2j+1} + n_{2j+4} = 1$ when each two-site lattice has exactly one fermion. One then finds

$$\underline{R}_X(\theta)_j = \exp\left(-i\underline{X}_j\frac{\theta}{2}\right) = \cos\left(\frac{\theta}{2}\right) - i\sin\left(\frac{\theta}{2}\right)(1 - 2n_{2j+2})(1 - 2n_{2j+3})\left(f_{2j+4}^\dagger f_{2j+1} + f_{2j+1}^\dagger f_{2j+4}\right).$$

One can write $\underline{Y}_j = -i\underline{Z}_j\underline{X}_j = iZ_{2j+1}\underline{X}_j$, so that the encoded \underline{Y} -rotation is

$$\underline{R}_Y(\theta)_j = \exp\left(-i\underline{Y}_j\frac{\theta}{2}\right) = \cos\left(\frac{\theta}{2}\right) + \sin\left(\frac{\theta}{2}\right)(1 - 2n_{2j+1})(1 - 2n_{2j+2})(1 - 2n_{2j+3})\left(f_{2j+4}^\dagger f_{2j+1} + f_{2j+1}^\dagger f_{2j+4}\right).$$

Finally, the encoded Hadamard gate is $\underline{H}_j = \underline{Z}_j\underline{R}_Y(-\pi/2)_j = -(1 - 2n_{2j+1})\underline{R}_Y(-\pi/2)_j$:

$$\underline{H}_j = \frac{1}{\sqrt{2}}\left[-1 + 2n_{2j+1} + (1 - 2n_{2j+2})(1 - 2n_{2j+3})\left(f_{2j+4}^\dagger f_{2j+1} + f_{2j+1}^\dagger f_{2j+4}\right)\right].\quad (10)$$

Note that in marked contrast with the qubit representation, in the fermion representation the \underline{X}_j , \underline{Y}_j , and \underline{H}_j operators acting on encoded qubit j (involving the two sites labeled by $2j + 1$ and $2j + 4$) are intrinsically non-local, since they depend explicitly on the fermion density at the intervening sites $2j + 2$ and $2j + 3$. Nevertheless they are fully separable (i.e. not entangling), as will be shown explicitly in the example below. One might ask why they are nevertheless non-local. Suppose that the $(1 - 2n_{2j+2})(1 - 2n_{2j+3})$ term were dropped in expression (9) for the encoded \underline{X}_j operator. The operation would then naïvely correspond to an unencoded X_j operation, but only in the absence of fermions between sites $2j + 1$ and $2j + 4$. If there were in fact one fermion occupying either of the intervening sites $2j + 2$ or $2j + 3$, then hopping between $2j + 1$ and $2j + 4$ would introduce undesired negative signs to certain matrix elements. Of course, these are exactly the factors that yield the ground-state entanglement in the first place! But they are unwanted in the implementation of X , Y , and H operations, and so need to be cancelled in the encoded versions \underline{X} , \underline{Y} , and \underline{H} if necessary. Consider two encoded qubits, for example. The basis is spanned

by the vectors $|1100\rangle = f_1^\dagger f_3^\dagger |\mathcal{O}_4\rangle$, $|1001\rangle = f_1^\dagger f_6^\dagger |\mathcal{O}_4\rangle$, $|0110\rangle = f_3^\dagger f_4^\dagger |\mathcal{O}_4\rangle$, and $|0011\rangle = f_4^\dagger f_6^\dagger |\mathcal{O}_4\rangle$, the encoded Hadamard gate (10) acting on the first encoded qubit is

$$\begin{aligned}\underline{H}_1 &= \frac{1}{\sqrt{2}}\begin{pmatrix} 1 & 0 & 1 & 0 \\ 0 & 1 & 0 & 1 \\ 1 & 0 & -1 & 0 \\ 0 & 1 & 0 & -1 \end{pmatrix} \\ &= \frac{1}{\sqrt{2}}(\underline{X} + \underline{Z}) \otimes \underline{I} = \underline{H} \otimes \underline{I},\end{aligned}\quad (11)$$

which is manifestly separable in matrix form even though it appears not to be in the fermion representation (10).

The measurements are made in the local fermion basis, so that

$$\begin{aligned}(\mathcal{M}_1)_j &= |\underline{0}\rangle_j \langle \underline{0}| = |1_{2j+1}0_{2j+4}\rangle \langle 1_{2j+1}0_{2j+4}| \\ &= f_{2j+1}^\dagger |\mathcal{O}_2\rangle_{2j+1,2j+4} \langle \mathcal{O}_2| f_{2j+1}\end{aligned}$$

and

$$\begin{aligned}(\mathcal{M}_2)_j &= |\underline{1}\rangle_j \langle \underline{1}| = |0_{2j+1}1_{2j+4}\rangle \langle 0_{2j+1}1_{2j+4}| \\ &= f_{2j+4}^\dagger |\mathcal{O}_2\rangle_{2j+1,2j+4} \langle \mathcal{O}_2| f_{2j+4}.\end{aligned}$$

In other words, the qubit projectors correspond simply to observing the site indexed by $2j + 1$ or $2j + 4$ to determine if a fermion is present; if so, it is projected into the encoded state $|\underline{0}\rangle$ or $|\underline{1}\rangle$, respectively.

B. Example: two-qubit gate teleportation

It is instructive to consider how one would implement one gate teleportation on a two-qubit fermionic cluster state. Suppose that the entire system consisted of sites 1, 3, 4, and 6 in Fig. 1(b) as in the two-qubit example in the previous section, with ground state given by Eq. (8). Suppose that all sources of energy exchange between the system and the environment are eliminated, other than those associated with applied rotations and measurements, so that $|\psi\rangle \equiv |\text{g.s.}\rangle$. In order to teleport an arbitrary single-qubit gate in a ordinary 1D cluster state, one needs to perform a series of measurements in the $HR_Z(\theta)$ basis. The first qubit is to be rotated first by the encoded gate $\underline{R}_Z(\theta)_1$, then by \underline{H}_1 , and then measured in the computational basis spanned by the states $|\underline{0}\rangle = f_1^\dagger |\mathcal{O}\rangle_{1,4}$ and $|\underline{1}\rangle = f_4^\dagger |\mathcal{O}\rangle_{1,4}$. Evidently the applied rotations on the first qubit will push $|\psi\rangle$ away from the ground state, though the fermions in all the other double wells remain in eigenstates of the original Hamiltonian. As a consequence, the state of the first qubit will oscillate at a frequency τ_{14}/\hbar . All states and operations can therefore be considered only at $2\pi/\tau_{14}$ intervals. This assumption is not essential, however, as discussed below in Sec. IV D.

A \underline{Z}_1 -rotation on the first encoded qubit yields

$$\begin{aligned} |\psi'\rangle &= \underline{R}_Z(\theta)|\psi\rangle = \frac{1}{2} \left(f_1^\dagger + e^{i\theta} f_4^\dagger \right) \left(f_3^\dagger + f_6^\dagger \right) |\mathcal{O}\rangle_{1,3,4,6} \\ &= \frac{1}{2} [|1100\rangle + |1001\rangle + e^{i\theta} (-|0110\rangle + |0011\rangle)]_{1,3,4,6}, \end{aligned}$$

ignoring an overall phase $e^{-i\theta/2}$; subsequent application of an encoded Hadamard operation gives

$$\begin{aligned} |\psi''\rangle &= \underline{H}_1|\psi'\rangle = \frac{1}{2\sqrt{2}} [(1 - e^{i\theta}) (|1100\rangle + |0011\rangle) \\ &\quad + (1 + e^{i\theta}) (|1001\rangle + |0110\rangle)]_{1,3,4,6}. \end{aligned}$$

Measurement of the first qubit in encoded state $|\underline{0}_1\rangle$ corresponds to the application of the projector $(\mathcal{M}_1)_1 = |1_1 0_4\rangle\langle 1_1 0_4| = f_1^\dagger |\mathcal{O}\rangle\langle \mathcal{O}| f_1$:

$$\begin{aligned} (\mathcal{M}_1)_1 |\psi''\rangle &= \frac{1}{2} [(1 - e^{i\theta}) |1100\rangle + (1 + e^{i\theta}) |1001\rangle] \\ &= \frac{1}{2} |\underline{0}_1\rangle [(1 - e^{i\theta}) |\underline{0}_2\rangle + (1 + e^{i\theta}) |\underline{1}_2\rangle] \\ &= \underline{H}_2 \underline{Z}_2 \underline{R}_Z(\theta)_2 |\underline{0}+\rangle. \end{aligned}$$

Likewise, applying the other projector $(\mathcal{M}_2)_1 =$

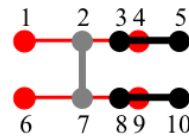


FIG. 2. (Color online) A subgraph of the two-dimensional leapfrog model, with the two overlapping sublattices corresponding to horizontal red (gray) and black links.

$|0_1 1_4\rangle\langle 0_1 1_4| = f_4^\dagger |\mathcal{O}\rangle\langle \mathcal{O}| f_4$ yields the state

$$\begin{aligned} (\mathcal{M}_2)_1 |\psi''\rangle &= \frac{1}{2} [(1 + e^{i\theta}) |0110\rangle + (1 - e^{i\theta}) |0011\rangle] \\ &= \frac{1}{2} |\underline{1}_1\rangle [(1 + e^{i\theta}) |\underline{0}_2\rangle + (1 - e^{i\theta}) |\underline{1}_2\rangle] \\ &= \underline{X}_2 \underline{H}_2 \underline{Z}_2 \underline{R}_Z(\theta)_2 |\underline{1}+\rangle. \end{aligned}$$

Thus, the gate teleportation using fermions proceeds exactly as in the usual spin-qubit case, though with an additional overall \underline{Z} operator reflecting the original ground state (8).

C. Two-dimensional cluster state

Though the Jordan-Wigner transformation is not uniquely defined in two dimensions, the structure of the qubit encoding carries naturally over to dimensions higher than one. A two-dimensional version of the leapfrog Hamiltonian is shown in Fig. 1(c). Two interpenetrating two-site lattices (shown in grey) that are staggered relative to each other are superimposed on an array of one-dimensional leapfrog chains, similar to those discussed above. Each double-well of the new lattices serves to connect adjacent one-dimensional chains, so the sites are situated between a given connected pair in the chains. Again, only a single fermion is allowed to occupy any given pair of sites of the new lattices. The labelling of the sites can be chosen in any convenient way. When writing out the full ground state in terms of the fermion field operators, one need only keep in mind which sites interleave others.

In order to demonstrate that the ground state of the fermionic leapfrog Hamiltonian is computationally universal, it remains to be shown that the presence of the vertical links has the effect of entangling the two horizontal chains. Consider for this purpose a two-dimensional subgraph of the full lattice configuration shown in Fig. 1(c), in which two encoded two-qubit cluster states are coupled together by a single vertical link as shown in Fig. 2. The sites on the top row are labeled 1 through 5 with site 2 the upper partner of the vertical double well, and the bottom three sites are labeled 5 through 10 with site 7 the lower partner of site 2. The Hamiltonian corresponding to this subgraph is

$$H_{2D} = -\tau \left(f_4^\dagger f_1 + f_5^\dagger f_3 + f_7^\dagger f_2 + f_9^\dagger f_6 + f_{10}^\dagger f_8 + \text{H.c.} \right).$$

It is simple to verify that the ground state is

$$|g.s.\rangle_{2D} = \frac{1}{\sqrt{32}} \left(f_1^\dagger + f_4^\dagger \right) \left(f_3^\dagger + f_5^\dagger \right) \left(f_2^\dagger + f_7^\dagger \right) \\ \times \left(f_6^\dagger + f_9^\dagger \right) \left(f_8^\dagger + f_{10}^\dagger \right) |\mathcal{O}\rangle.$$

If the vertical link (sites 2 and 7) truly entangles the two horizontal chains, then measuring the fermions in all the double wells labeled by $\{1, 4\}$, $\{6, 9\}$, and $\{2, 7\}$ should yield entanglement between the two encoded qubits associated with the double wells labeled by $\{3, 5\}$ and $\{8, 10\}$, even though there is no explicit link remaining between them. The $\{1, 4\}$ and $\{6, 9\}$ sites are measured in the encoded X basis, corresponding to the application of an encoded Hadamard gate followed by a computational-basis measurement. The $\{2, 7\}$ sites are measured in the encoded Y basis, i.e. the $\{2, 7\}$ sites are first transformed by \sqrt{X} and then measured in the computational basis. The result doesn't depend on the order in which these operations and measurements are made, because only Pauli byproduct operators are teleported. Ignoring overall phases the output is

$$|\text{out}\rangle = |m_1 m_2 m_3\rangle_{1,2,4,6,7,9} \\ \otimes \left[\underline{a}_{12} \underline{H}_1 \sqrt{\underline{Z}_1} \underline{H}_2 \sqrt{\underline{Z}_2} \underline{CZ}_{12} |++\rangle \right]_{3,5,8,10},$$

where $m_i = \{0, 1\}$ are the measurement outcomes and

$$\underline{a}_{12} = \{ \underline{X}_1, \underline{X}_2, \underline{Z}_2, \underline{X}_1 \underline{Y}_2, \underline{Y}_1 \underline{X}_2, \underline{Z}_1, \underline{Z}_1 \underline{Y}_2, \underline{Y}_1 \underline{Z}_2 \}$$

are local encoded Pauli byproduct operators corresponding to the eight possible outcomes. Thus, the result of these measurements is to maximally entangle the two qubits $|+\rangle_{3,5}$ and $|+\rangle_{8,10}$. If the two qubits encoded on sites $\{1, 4\}$ and $\{6, 9\}$ were originally in the states $|\underline{\psi}_1\rangle$ and $|\underline{\psi}_2\rangle$, then the result would be the same as that above except with $|++\rangle_{3,5,8,10} \rightarrow |\underline{\psi}_1 \underline{\psi}_2\rangle_{3,5,8,10}$.

D. Practical Considerations

The two-qubit example demonstrates how one-dimensional fermionic cluster states can be used in order to perform universal gate teleportation. Nevertheless, it is not apparent how the various encoded operations — the $\underline{R}_Z(\theta)$, \underline{H} , $\underline{R}_X(\pi/2) = \sqrt{X}$, and measurements — would be implemented in practice. Of particular concern is that the encoded Hadamard gate and the \underline{X} and \underline{Y} rotations are explicitly non-local in the fermion representation, as shown above [cf. Eqs.(9) and (10)]: all require local hopping on a given pair of sites in a sublattice with an amplitude dependent on the occupancy of intervening qubits on different sublattices. As shown below, it is possible to implement all encoded operations but only if one allows the fermions to explicitly interact.

Consider again the two-qubit example discussed above. All local gates on the first qubit can be performed by the

application of the additional two-site hopping Hamiltonians

$$\hat{H}_a(\tau_{14}, V_1, V_4) = \tau_{14} \left(f_4^\dagger f_1 + f_1^\dagger f_4 + V_1 n_1 + V_4 n_4 \right) \quad (12)$$

and

$$\hat{H}_b(\tau_{34}, g, V_3, V_4) = \tau_{34} \left(f_{4,\sigma}^\dagger f_{3,\sigma} + f_{3,\sigma}^\dagger f_{4,\sigma} + g n_{3,\sigma} n_{3,\sigma'} \right. \\ \left. + V_3 n_{3,\sigma} + V_4 n_{4,\sigma} \right), \quad (13)$$

for particular choices of parameters and times. The Hamiltonian (12) is the same as Eq. (4), with the addition of potential energies V_1 and V_4 on the two sites of the first double-well. The spin indices σ and σ' in Hamiltonian (13) represent the fermionic spin projection for encoded qubits 1 and 2, respectively. Thus, the fermion encoding qubit 1 is allowed to tunnel between sites 4 and 3 and possibly interact with the inert fermion on site 3.

A fermion may or may not be present on site 3 (if not, then it occupies site 6), so the Hamiltonians (12) and (13) act on two independent two-dimensional blocks. For H_a , the states in the first block are $\{ f_1^\dagger f_4^\dagger |\mathcal{O}\rangle, f_3^\dagger f_4^\dagger |\mathcal{O}\rangle \}$, while those in the second block are $\{ f_1^\dagger |\mathcal{O}\rangle, f_4^\dagger |\mathcal{O}\rangle \}$. In the first block, a fermion hopping between sites 1 and 4 must cross the fermion in site 3, acquiring a negative sign in the process; the sign change is absent in the second block. But all single-qubit operations on the first qubit must be truly local: the resulting gate $\exp(-itH)$ cannot depend on the state of the second qubit, i.e. the possible presence of a fermion on site 3. For H_b , the two states in the first block correspond to $\{ f_{3,\sigma'}^\dagger f_{3,\sigma}^\dagger |\mathcal{O}\rangle, f_{3,\sigma'}^\dagger f_{4,\sigma}^\dagger |\mathcal{O}\rangle \}$, while those in the second block are $\{ f_{3,\sigma}^\dagger |\mathcal{O}\rangle, f_{4,\sigma}^\dagger |\mathcal{O}\rangle \}$. No fermions cross in either block, but additional phases can result from the interaction in site 3 of a fermion with spin σ and one with spin σ' .

The most straightforward gate is an arbitrary Z -axis rotation on the first qubit, which corresponds to turning on H_a for a given time: $\underline{R}_Z(-V_4 t)_1 = \exp[-itH_a(0, 0, V_4)]$ for either block, ignoring an overall unimportant phase. In practise, a strong repulsive potential would be applied to the barrier between sites 1 and 4 to turn off tunneling, and another potential applied to site 4. Next consider the implementation of the encoded Hadamard gate \underline{H}_1 . Applying $H_a(\tau_{14}, -1 + \sqrt{2}, 1 + \sqrt{2})$ for a time $t = \pi/\sqrt{8}\tau_{14}$ yields \underline{H}_1 in the first block and $\underline{Z}_1 \underline{H}_1 \underline{Z}_1$ in the second. This gate is equivalent to $\underline{CZ}_{12} \underline{H}_1 \underline{CZ}_{12}$ which is not the desired Hadamard gate. Likewise, the application of $H_a(\tau_{14}, 0, 0)$ for a time $t = \pi/4\tau_{14}$ yields $\underline{CZ}_{12} \underline{R}_X(\pi/2)_1 \underline{CZ}_{12}$ rather than $\underline{R}_X(\pi/2)_1$. In order to obtain the desired gates, one can apply H_b both before and after the H_a above. Choosing $H_b\left(\tau_{34}, \frac{4}{\sqrt{3}}, -\frac{1}{\sqrt{3}}, \frac{1}{\sqrt{3}}\right)$ for a time $t = \sqrt{3}\pi/2\tau_{34}$ yields \underline{I}_1 in the first block and \underline{Z}_1 in the second, i.e. the gate \underline{CZ}_{12} . All parameters in H_a are assumed to be zero during the operation of H_b . Because H_b also applies a possible phase

to the first register of the second qubit, a repulsive σ' potential should be applied between sites 4 and 6 during its application and removed thereafter. The majority of the state thereby remains in the ground state of the primary governing Hamiltonian.

It is interesting to note that any attempt to perform a local operation U_1 within the initial non-interacting fermionic model instead yields $CZ_{12}U_1CZ_{12}$, which is a two-qubit matchgate modulo local operations. For example, attempting $U_1 = H_1$ produces a maximally entangling gate that is locally unitary-equivalent to the matchgate G_{HH} [26]. In order to obtain a true local operation, required for universal MBQC when restricted to computational basis measurements, one must include some kind of fermion-fermion interaction. In the approach above, an additional hopping Hamiltonian with an on-site interaction yields an explicit CZ_{12} which can cancel the effective CZ_{12} arising solely from fermionic statistics. Because one can construct the SWAP gate from combinations of Hadamards and CZ gates, this approach is the measurement-based analogue of the fermionic circuit model found previously [22].

V. DISCUSSION AND CONCLUSIONS

Through the ‘leapfrog’ model of fermions hopping across one another in a lattice, statistical antisymmetry and entanglement are shown to be equivalent quantities in fermionic systems. As a result, the ground state has maximal entanglement between all neighboring qubits, which is inherently insensitive to decoherence as long as the temperature remains lower than the energy gap. In principle, such a resource could be used for a variety of

distributed quantum information protocols. Yet, universal MBQC using this resource is impossible under a realistic model where only computational basis measurements are allowed. A universal set of gates can be obtained only when an additional local Hamiltonian is added that allows the fermions to explicitly interact through collisions. Note also that any double-well sites with zero or two fermions behave as defects (holes) in the cluster state; universal quantum computation is still possible as long as connectivity of the state exceeds the percolation threshold [48].

The results suggest that the ground states of interacting fermionic systems could generically be resources for quantum information processing within the MBQC framework. One requires only that the constituent fermionic wavefunctions have the opportunity to overlap one another, and interact in the process. Because these criteria arguably apply to almost all physical systems, discovering other suitable candidate Hamiltonians might be relatively straightforward, though finding convenient encodings for the quantum information might still pose a significant challenge.

ACKNOWLEDGMENTS

I would like to thank Aephraim Steinberg, Jens Eisert, and Gora Shlyapnikov for stimulating discussions. I am particularly grateful to the hospitality of the Laboratoire de Physique Théorique et Modèles Statistiques at the Université de Paris-Sud where the main ideas were worked out. This work was supported by the Natural Sciences and Engineering Research Council of Canada.

-
- [1] H. J. Briegel, D. E. Browne, W. Dur, and R. Raussendorf, and M. Van den Nest, *Nat. Phys.* **5**, 19 (2009).
 - [2] R. Raussendorf, D. E. Browne, and H. J. Briegel, *Phys. Rev. A* **68**, 022312 (2003).
 - [3] M. Van den Nest, K. Luttmner, W. Dur, and H. J. Briegel, *Phys. Rev. A* **77**, 012301 (2008).
 - [4] M. Fannes, B. Nachtergaele, and R. F. Werner, *Commun. Math. Phys.* **144**, 443 (1992).
 - [5] F. Verstraete and J. I. Cirac, *Phys. Rev. A* **70**, 060302 (2004).
 - [6] D. Perez-Garcia, F. Verstraete, M. M. Wolf, and J. I. Cirac, *Quantum Inf. Comput.* **7**, 401 (2007).
 - [7] D. Gross, J. Eisert, N. Schuch, and D. Perez-Garcia, *Phys. Rev. A* **76**, 052315 (2007).
 - [8] J.-M. Cai, W. Dür, M. Van den Nest, A. Miyake, and H. J. Briegel, *Phys. Rev. Lett.* **103**, 050503 (2009).
 - [9] C. E. Mora et al., *Phys. Rev. A* **81**, 042315 (2010).
 - [10] D. Gross, S. T. Flammia, and J. Eisert, *Phys. Rev. Lett.* **102**, 190501 (2009).
 - [11] M. J. Bremner, C. Mora, and A. Winter, *Phys. Rev. Lett.* **102**, 190502 (2009).
 - [12] X. Chen, B. Zeng, Z.-C. Gu, B. Yoshida, and I. L. Chuang, *Phys. Rev. Lett.* **102**, 220501 (2009).
 - [13] I. Affleck, T. Kennedy, E. H. Lieb, and H. Tasaki, *Commun. Math. Phys.* **115**, 477 (1988).
 - [14] A. Miyake, *Ann. Phys.* **326** 1656 (2011).
 - [15] T. C. Wei, I. Affleck, and R. Raussendorf, *Phys. Rev. Lett.* **106**, 070501 (2011).
 - [16] C. W. J. Beenakker, D. P. DiVincenzo, C. Emary, and M. Kindermann, *Phys. Rev. Lett.* **93**, 020501 (2004).
 - [17] E. Knill, R. Laflamme, and G. J. Milburn, *Nature* **409**, 46 (2001).
 - [18] X. L. Zhang, M. Feng, and K. L. Gao, *Phys. Rev. A* **73**, 014301 (2006).
 - [19] L. Amico, R. Fazio, A. Osterloh, and V. Vedral, *Rev. Mod. Phys.* **80**, 517 (2008).
 - [20] J. Eisert, M. Cramer, and M. B. Plenio, *Rev. Mod. Phys.* **82**, 277 (2010).
 - [21] T. Barthel, C. Pineda, and J. Eisert, *Phys. Rev. A* **80**, 042333 (2009).
 - [22] R. Jozsa, B. Kraus, A. Miyake, and J. Watrous, *Proc. Roy. Soc. A* **466**, 809 (2010).

- [23] C. V. Kraus, N. Schuch, F. Verstraete, and J. I. Cirac, Phys. Rev. A **81**, 052338 (2010).
- [24] I. Pizorn and F. Verstraete, Phys. Rev. B **81** 245110 (2010).
- [25] L. G. Valiant, SIAM J. Comput. **31**, 1229 (2002).
- [26] S. Ramelow, A. Fedrizzi, A. M. Steinberg, and A. G. White, New J. Phys. **12** 083027 (2010).
- [27] I. Bloch, Nat. Phys. **1**, 23 (2005).
- [28] O. Morsch, and M. Oberthaler, Rev. Mod. Phys. **78**, 179 (2006).
- [29] O. Mandel *et al.*, Phys. Rev. Lett. **91**, 010407 (2003).
- [30] O. Mandel *et al.*, Nature **425**, 937 (2003).
- [31] D. Jaksch, and P. Zoller, Ann. Phys. **315**, 52 (2005).
- [32] P. J. Lee *et al.*, Phys. Rev. Lett. **99**, 020402 (2007).
- [33] M. Anderlini, *et al.*, Nature **448**, 452 (2007).
- [34] G. de Chiara *et al.*, Phys. Rev. A **77**, 052333 (2008).
- [35] S. Folling *et al.*, Nature **448**, 1029 (2007).
- [36] S. Trotzky, *et al.*, Science **319**, 295 (2008).
- [37] T. B. Ottenstein *et al.*, Phys. Rev. Lett. **101**, 203202 (2008).
- [38] J. R. Williams, *et al.*, Phys. Rev. Lett. **103**, 130404 (2009).
- [39] G. Modugno *et al.*, Phys. Rev. A **68**, 011601 (2003).
- [40] M. Köhl *et al.*, Phys. Rev. Lett. **94**, 080403 (2005).
- [41] R. Jordens *et al.*, Nature **455**, 204 (2008).
- [42] J. K. Chin *et al.*, Nature **443**, 961 (2006).
- [43] Y. R. P. Sortais *et al.*, Phys. Rev. A **75**, 013406 (2007).
- [44] K. Nelson, X. Li, and D. S. Weiss, Nat. Phys. **3**, 556 (2007).
- [45] J. Beugnon *et al.*, Nat. Phys. **3**, 696 (2007).
- [46] M. Karski *et al.*, Phys. Rev. Lett. **102**, 053001 (2009).
- [47] W. S. Bakr *et al.*, Nature **462**, 74 (2009).
- [48] K. Kieling, T. Rudolph, J. Eisert, Phys. Rev. Lett. **99**, 130501 (2007).